Proceedings of the 7th International Conference on Signal Processing and Machine Learning
DOI: 10.54254/2755-2721/2027.39074

Analysis of Spatiotemporal Patterns and Influencing Factors of Soil Erosion in Southeastern Hubei Based on the RUSLE Model

Shuxian Li

School of Urban and Environmental Sciences, Hubei Normal University, Huangshi, China
2017400892@qq.com

Abstract. High-standard agricultural development constitutes a core strategic approach to safeguarding national food security and realizing agricultural modernization, yet soil erosion imposes severe threats to food security and sustainable agricultural development. Based on multi-temporal remote sensing datasets and the RUSLE model, this study quantitatively evaluates the spatiotemporal variations in soil erosion across Southeastern Hubei from 1998 to 2020. A soil erosion transition matrix is adopted to characterize the conversion among erosion grades and identify the drivers behind spatial heterogeneity and erosion magnitude.The results reveal that precipitation, slope length and steepness, vegetation coverage and land-use type are the primary influencing factors of soil erosion in the study area. This work clarifies the erosion-mitigation effects of different anthropogenic factors and optimizes relevant governance countermeasures, highlighting the prominent role of precipitation in regulating soil erosion processes.Elucidating the controlling factors of soil erosion intensity provides scientific support for regional soil and water conservation practices. Moreover, it facilitates precision agricultural management under multi-source data integration, improves farmland production efficiency, and further promotes the development of smart agriculture.

Keywords: Soil erosion, RUSLE, Land use, Southeastern Hubei

1. Introduction

Soil erosion is a common global eco-environmental problem. It reduces soil thickness, fertility and land productivity, and causes sediment accumulation and floods, threatening regional food, ecological and socio-economic security. Southern China's hilly red soil region has abundant heat and rainfall. However, hilly terrain, concentrated rainstorms and human activities such as mining and urban expansion make it prone to soil erosion, creating tough challenges for erosion control.

The Revised Universal Soil Loss Equation (RUSLE), a classic model for soil erosion quantification, is widely adopted in China for erosion modulus estimation and spatiotemporal analysis owing to its simple principles and accessible parameters [1]. Existing studies on Hubei's soil erosion mainly focus on its southwest and northwest mountain areas. Few researches concern the long-term erosion evolution and driving factors in the low-hill transition zone of Wuhan

© 2026 The Authors. This is an open access article distributed under the terms of the Creative Commons Attribution License 4.0 (https://creativecommons.org/licenses/by/4.0/).

DOI: 10.54254/2755-2721/2027.39074

metropolitan area in southeastern Hubei. As a populous and fast-urbanizing hilly region, southeastern Hubei faces prominent conflicts among urban expansion, mine restoration, agriculture and ecological conservation [2]. Exploring soil erosion evolution from 1998 to 2020 and quantifying effects of precipitation, terrain, soil, vegetation and conservation measures can support local erosion management, ecological restoration and farmland protection.

This study selects Wuhan, Xianning, Ezhou and Huangshi in southeastern Hubei as the study area. Based on multi-source data (remote sensing images, DEM, soil, meteorology and land use), RUSLE is used to calculate soil erosion modulus from 1998 to 2020. We analyze the temporal and spatial patterns of erosion intensity, examine influences of each factor, identify dominant drivers and locate key erosion control zones. The results provide theoretical and data support for soil loss governance, environmental protection and precision agriculture in southeastern Hubei.

2. Data and methods

2.1. Study-area description

As shown in Figure 1, Southeastern Hubei, covering Wuhan, Xianning, Ezhou and Huangshi, has a total land area of approximately 20 000 km².As a geomorphic transition zone between the Mubu Mountains and Jianghan Plain, its terrain gradually decreases from south to north, consisting of three geomorphic units: middle mountains of the northern Mubu Mountains, the Damu-Yushan low mountain-hill zone, and the Jianghan lacustrine-alluvial plain.

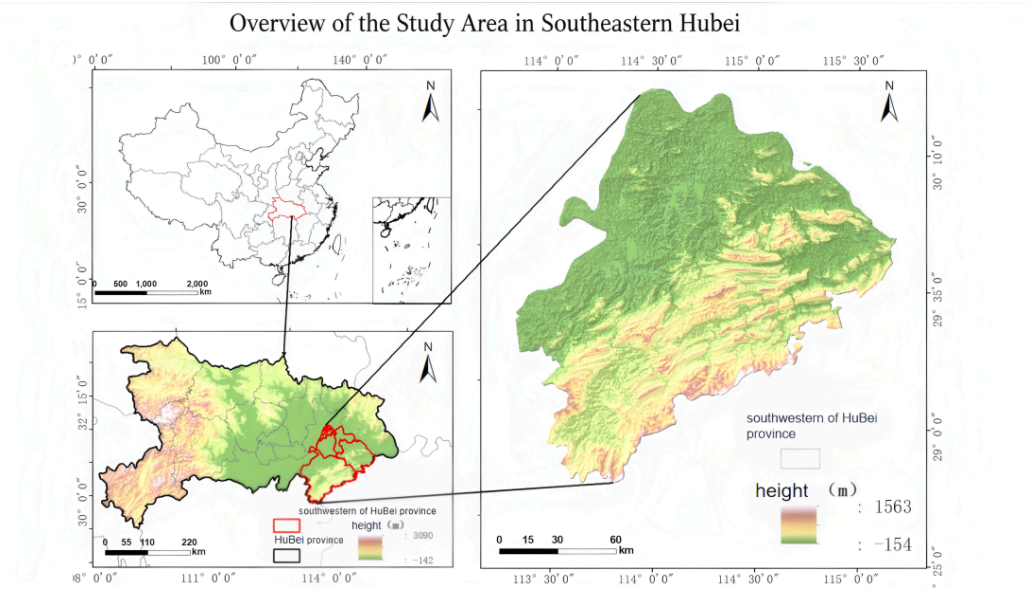

Figure 1. Overview of the study area

The study area has a humid subtropical monsoon climate with distinct seasons and hot-rainy synchronization. It belongs to Hubei's high-precipitation zone, with annual precipitation of 1300–1690 mm. Precipitation exceeds evaporation, maintaining high soil moisture. Zonal vegetation shifts from evergreen broad-leaved forests to low-hill secondary vegetation [3]. Rainfall concentrates from May to September with persistent heavy rain. Dominated by low mountains and hills, this region faces severe soil erosion due to historical mining and heavy industry. Since 1998, climate change has increased extreme rainstorms and erosion risks. Meanwhile, ecological projects such as the

DOI: 10.54254/2755-2721/2027.39074

Grain-for-Green Program and mine restoration have altered local land use. Combined natural and human factors create complex spatiotemporal heterogeneity in regional soil erosion.

2.2. Quantification of soil-erosion factors

The Revised Universal Soil Loss Equation (RUSLE) quantifies soil erosion modulus using multiple factors: rainfall, soil type, vegetation cover and soil-water conservation practices. With solid theoretical basis, low data demand and readily available multi-source datasets, RUSLE is a mature and widely used model for soil erosion assessment.The core RUSLE formula is as follows:

$$A = R \times K \times LS \times C \times P \tag{1}$$

where A is the soil-erosion modulus (t/hm²·a) R is the rainfall-erosivity factor (MJ·mm/(hm²·h·a)), K is the soil-erodibility factor (t·hm²·MJ·mm)), LS denotes the topographic factor (where L represents the slope-length factor and S represents the slope-steepness factor) C is the vegetation-cover-management factor, and P is the support-practice factor for soil and water conservation.

(1) Rainfall-erosivity factor (R)

The rainfall erosivity factor quantifies rainfall's capacity to trigger soil erosion. Many validated algorithms are available for its estimation across China. These linear or nonlinear empirical equations are built from rainfall intensity, kinetic energy, or annual, monthly and daily precipitation data. This study uses a simplified empirical method based on monthly average precipitation to calculate rainfall erosivity in southeastern Hubei.

$$R = 0.3589F^{1.9462} \tag{2}$$

$$F = \sum_{i=1}^{12} P_j^2 \tag{3}$$

Where F represents an index characterizing the seasonal distribution of precipitation relevant to soil erosion (unit: mm); P andP_i denote the annual precipitation and total precipitation of the i-th month, respectively.

(2) Determination of the soil-erodibility factor (K)

The soil erodibility factor K is a core parameter in soil erosion models, representing soil's inherent susceptibility to erosion. K calculation methods are selected according to available local soil property data [4]. Its value is mainly determined by soil particle composition, organic carbon content, soil structure and topsoil permeability. This study adopts the widely applicable EPIC model to compute K values. Soil classification and property datasets were obtained from the official website of the Nanjing Institute of Soil Science, Chinese Academy of Sciences. The formula is shown below:

$$K_{EPIc} = 0.1317\{0.2 + 0.3\exp[-0.025\,6San(1 - \tfrac{Sil}{100})]\} \tag{4}$$

$$\times(\tfrac{Sil}{Cla+Sil})^{0.3}[1 - \tfrac{0.25OC}{OC+\exp(3.72-2.95OC)}] \times [1 - \tfrac{0.7Sn}{Sn+\exp(-5.51+22.9Sn)}]$$

$$K = 0.51575K_{EPIC} - 0.01383 \tag{5}$$

DOI: 10.54254/2755-2721/2027.39074

Where K_{EPIC}denotes the soil-erodibility factor computed using the *EPIC* model. *Sil,Cla*and *San*represent the silt,clay, and sand particle contents in soil, respectively;*OC* refers to soil organic-carbon content. All these variables are expressed in percentage. *Sn* stands for a constant coefficient.

(3) Calculation of slope-length and slope-steepness factors (LS)

The topographic factor LS combines slope length and slope gradient, two geomorphic variables controlling rainfall-triggered soil erosion. RUSLE considers sediment deposition and slope-angle effects; erosion intensity typically rises with steeper slopes. Here, the LS factor was extracted from the Digital Elevation Model (DEM) [5]. The 30 m ASTER GDEM, downloaded from the National Geospatial Data Cloud Platform, was resampled as the final DEM [6]. Traditional slope algorithms perform best for gradients of 0°–18°, and most slopes in southeastern Hubei fall within this range. Thus, the LS calculation tool proposed by Zhang et al [7]. was used to generate continuous LS grids for the study area.

$$S = \begin{cases} 10.8\sin\theta + 0.03, & \theta < 5^\circ \\ 16.8\sin\theta - 0.50, & 5^\circ \le \theta < 10^\circ \\ 21.9\sin\theta - 0.96, & \theta \ge 10^\circ \end{cases} \tag{6}$$

$$L = \left(\frac{\lambda}{22.1}\right)^m \tag{7}$$

$$m = \begin{cases} 0.2, & \theta \le 1^\circ \\ 0.3, & 1^\circ < \theta \le 3^\circ \\ 0.4, & 3^\circ < \theta \le 5^\circ \\ 0.5, & \theta > 5^\circ \end{cases} \tag{8}$$

where S denotes the slope-steepness factor; θ is the slope gradient (°); L represents the slope-length factor; λ stands for the field slope length (m); and m is the slope-length exponent.

(4) Determination of vegetation-cover-management factor (C)

The vegetation-cover-management factor C, which is partly controllable via human activities, is determined by surface vegetation types and land-use conditions. Sentinel-2 land-use datasets were resampled to generate raster data with a spatial resolution of 10 m. In this study, land-use types in southeastern Hubei were classified into grassland, cropland, forest, built-up area, and water body. Different tillage practices and land-management modes exert influences on C values, which generally range from 0 to 1. Fractional vegetation cover (f_c) was estimated using a conversion model based on the Normalized Difference Vegetation Index (NDVI) [8]. The C factor was further calculated through the regression function between fractional vegetation cover and C. The corresponding equations are given as follows:

$$NDVI = f_c \times NDVI_{max} + (1 - f_c) \times NDVI_{min} \tag{9}$$

$$f_c = \frac{NDVI - NDVI_{min}}{NDVI_{max} - NDVI_{min}} \tag{10}$$

$$C = \begin{cases} 1, & (f_c = 0) \\ 0.6508 - 0.0436\lg f_c, & (0 < f_c \le 78.3\%) \\ 0, & (78.3 > f_c) \end{cases} \tag{11}$$

DOI: 10.54254/2755-2721/2027.39074

where C represents the vegetation-cover-management factor; f_c is the fractional vegetation cover within each pixel. $NDVI_{max}$ and $NDVI_{min}$ correspond to the NDVI values at the 95 % and 5 % cumulative percentiles, respectively. Nevertheless, Sentinel-2 observations have been available only since 2014. To reconstruct historical NDVI records, a bivariate linear regression model was established based on the relationship between NDVI and precipitation [9]. This model was adopted to estimate historical NDVI time-series and further derive C values for the period from 1998 to 2014.

(5) Determination of support-practice factor (P)

The support-practice factor P is defined as the ratio of soil loss under specific soil-water conservation measures to the soil loss occurring at the same site without such conservation interventions under identical environmental conditions. Common conservation measures include terracing and optimized cultivated-land management. In this study, datasets of HYDE 3.2.1 and CCI-LC from the Gee data repository were overlaid to assign P values ranging from 0 to 1 for different land-use categories. Drawing on the previous study conducted by Sun et al. [10] in Lichuan City, P values were assigned as follows: cropland 0.2, grassland 0.8, water body 0, built-up land 0.1, unused land 1, and forest 1. As shown in Table 1, the P factor is a dimensionless parameter ranging from 0 to 1. According to the definition of P, lower P values indicate more effective soil-water conservation, whereas higher P values correspond to more severe soil-loss risks [3].

Table 1. Summary of water and soil conservation factors by different land types

Land-use type	Grassland	Forest	Cropland	Water body	Built-up land	Unused land
P value	0.8	1	0.2	0	0.1	1

2.3. Classification of soil-erosion intensity

According to the Standards for Classification and Gradation of Soil Erosion (SL 190-2007) issued by the Ministry of Water Resources of China, soil erosion in the study area was classified into six grades based on soil-erosion modulus. Under this national standard, slight erosion corresponds to soil loss less than 200 $t \cdot km^{-2} \cdot a^{-1}$; light erosion ranges from 200 to 2500 $t \cdot km^{-2} \cdot a^{-1}$; moderate erosion ranges from 2500 to 5000 $t \cdot km^{-2} \cdot a^{-1}$; strong erosion ranges from 5000 to 8000 $t \cdot km^{-2} \cdot a^{-1}$; very-strong erosion ranges from 8000 to 15000 $t \cdot km^{-2} \cdot a^{-1}$; and severe erosion exceeds 15000 $t \cdot km^{-2} \cdot a^{-1}$.

Nevertheless, the soil-erosion modulus A output from the RUSLE model adopts the unit of $t \cdot km^{-2} \cdot a^{-1}$; Accordingly, six erosion-intensity grades were defined for this study: slight erosion (0~200 t/ ($km^2 \cdot$ a)), light erosion (200 ~ 2500t/($km^2 \cdot$ a)), moderate erosion (2 500 ~ 5000t/(km2· a)), strong erosion (5000 ~ 8000t/($km^2 \cdot$a)), very-strong erosion (8000 ~ 15000t/($km^2 \cdot$a)), and severe erosion (>15000t/($km^2 \cdot$a)).

3. Results and analysis

3.1. Variation characteristics of individual soil-erosion factors

3.1.1. Relationships between soil erosion and slope gradient

Slope gradient exerts a fundamental control over soil-erosion processes [11]. Erosion potential rises as terrain gradient increases. According to the topographic conditions of southeastern Hubei, slopes within the study area were classified into six groups by the natural-breaks classification method: 0-

DOI: 10.54254/2755-2721/2027.39074

2°, 2-4°, 4-7°, 7-10°, 10-18°, and >18°. The soil-erosion-modulus raster was overlaid with the slope-gradient raster to calculate the mean area of each soil-erosion intensity for every slope class across five epochs: 2000, 2005, 2010, 2015 and 2020.

As shown in Figure 2 which shows the slope-gradient map of the study area, the land area corresponding to each slope class decreases with increasing slope magnitude. Macroscopically, terrain across southeastern Hubei is highly heterogeneous. The southern part features rugged and undulating landforms, whereas the northwestern and central regions are relatively stable, dominated by gentle and nearly flat terrain. Slope values across the whole region range broadly from 0.03° to 18.98°. Meanwhile, Figure 3 which shows the slope-length map indicates generally low slope-length values within the study area, with a narrower value range of 0-11.64 compared with slope gradient. Patches with high slope-length values are scattered throughout the study domain; zones with relatively large slope-length are concentrated in the southeast and exhibit a zonal distribution pattern.

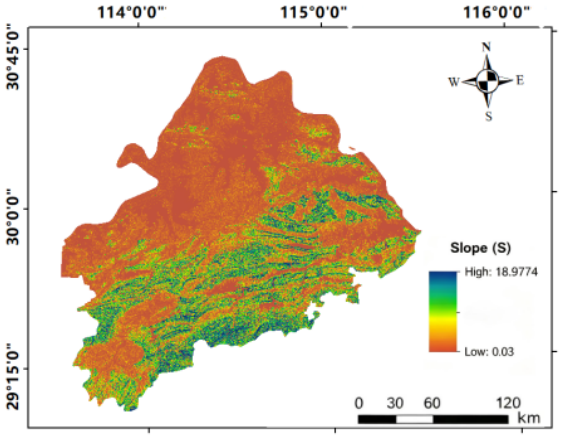

Figure 2. Slope diagram of the study area

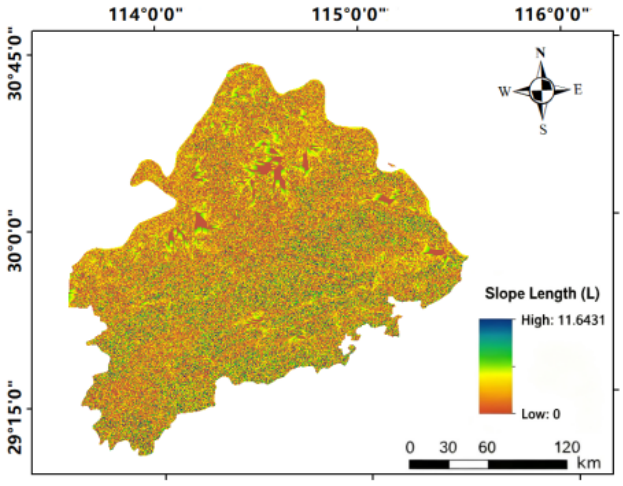

Figure 3. Schematic diagram of slope lengths in the study area

3.1.2. Soil-erosion variations under different land-use types

Based on land-use raster data, the spatial pattern of the support-practice factor (P) stayed relatively stable during 2000–2020. According to the assignment criteria in Table 1, low P values appeared in the northwest and south of southeastern Hubei (Wuhan, Huangshi and Ezhou), where water bodies, cropland and built-up land occupy large areas. In comparison, the southwest, central and southern zones had much higher P values, mainly covered by unused land, forest and grassland.

Temporally, high-value P areas concentrated in the south in 2000. Cropland spread widely across the whole study area, large water bodies clustered in the northwest and small water bodies scattered elsewhere. The overall spatial pattern of P did not change greatly in 2005, 2010, 2015 and 2020. However, forestland gradually expanded and replaced cropland in many places due to the Grain-for-Green Program. Hubei carried out this national ecological project starting in 2000 and launched a new phase in 2014. Over two decades, the program restored 1.77546 million mu of land in Hubei, benefiting 6.57 million residents from 1.71 million households in 95 counties [12]. Meanwhile,

DOI: 10.54254/2755-2721/2027.39074

boosted by the Wuhan-centered urban agglomeration, satellite city construction and Ezhou's airport economy, built-up land expanded outward radially from Wuhan.

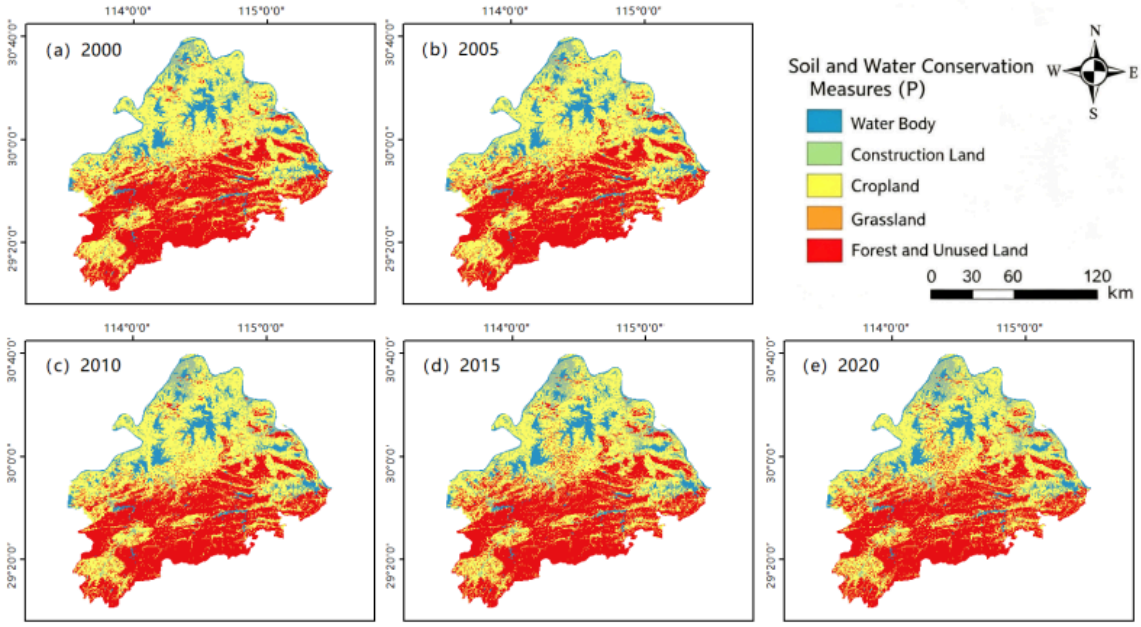

Figure 4. Schematic diagram of soil and water conservation measures in the study area

3.1.3. Spatiotemporal impacts of rainfall-erosivity intensity on soil erosion

As illustrated in the figure 5, the rainfall erosivity factor (R) of southeastern Hubei rose greatly from 2000 to 2010 and decreased after peaking in 2010. Spatially, Xianning and Huangshi were persistent hotspots of high rainfall erosivity, especially northeastern Xianning, southeastern Huangshi and their border regions. Meanwhile, the R values in the northwest of the study area also increased obviously during the research period.

Numerical analysis shows that the maximum rainfall erosivity was 6589.97 mm in 2000 and climbed to 7985.11 mm in 2005. The factor reached an unprecedented peak in 2010: its maximum and mean values almost tripled compared with 2005, with the maximum value of 25228.6 mm and mean value increasing from 180 mm to 530 mm. Meteorological data indicate that 2010 had heavy summer torrential rain and the maximum annual precipitation of 2802.48 mm. Influenced by the severe floods in Hubei and Hunan during 1998–1999, precipitation in 2000 stayed relatively low, resulting in weak rainfall erosivity. Although R declined in 2015 and 2020, its overall erosion potential remained higher than the pre-2010 level.

In summary, rainfall-related erosion risk gradually intensified. With concentrated rainfall, Huangshi and Xianning faced stronger rainfall impacts than other cities in southeastern Hubei. This result reflects growing extreme rainstorms and flash floods over the past two decades, which have increased rainfall erosivity and soil loss risks in this region.

DOI: 10.54254/2755-2721/2027.39074

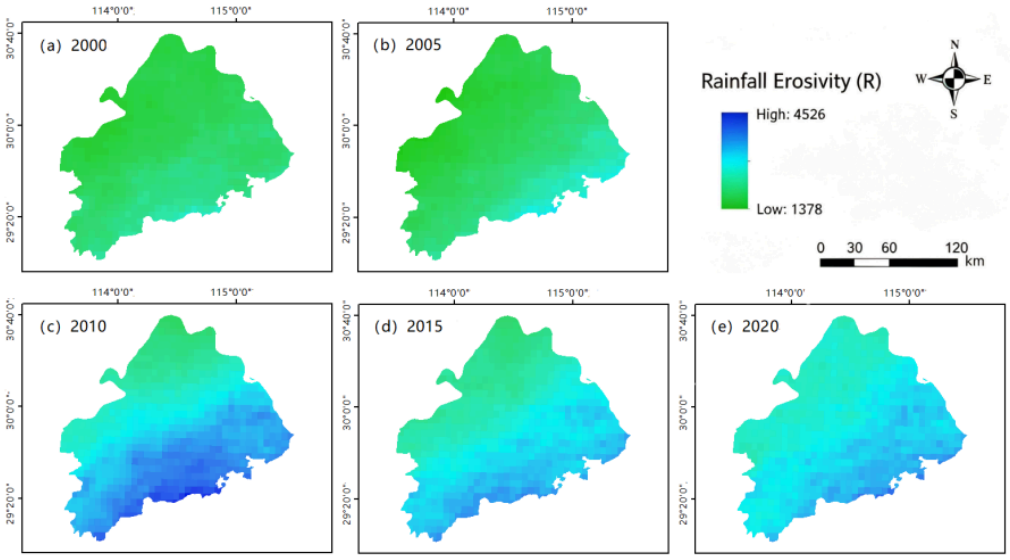

Figure 5. Schematic diagram of rainfall erosion factor in the study area

3.1.4. Impacts of fractional vegetation cover on soil erosion

As shown in the figure, fractional vegetation cover in southeastern Hubei shows a zonal clustered spatial pattern. Vegetation cover is low in the northwest and high in central and southern areas, with low-cover belts between these two regions. Ezhou and Wuhan have lower vegetation cover compared with Huangshi and Xianning.

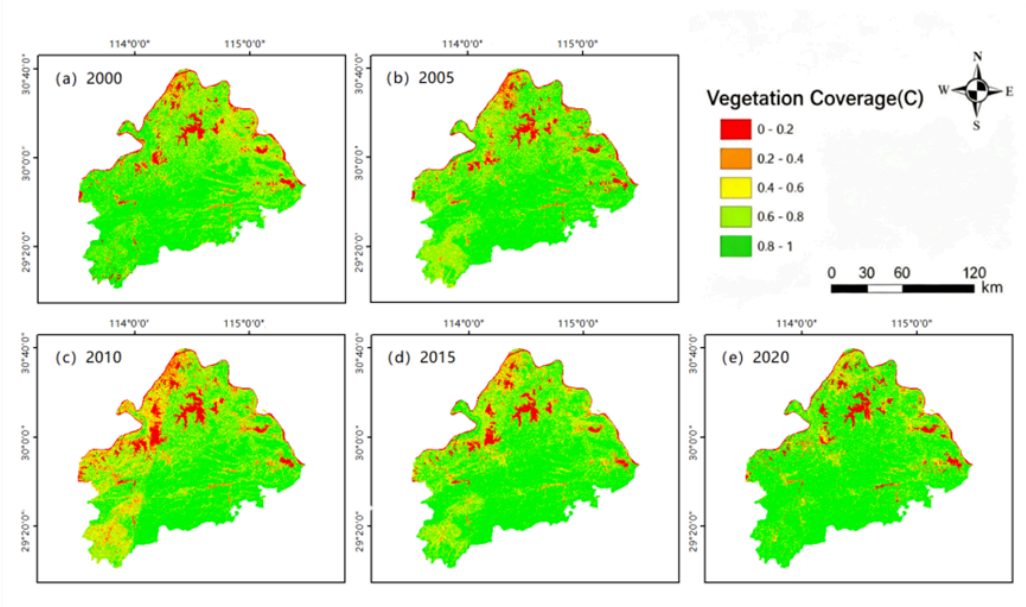

Figure 6. Schematic diagram of vegetation cover factors in the study area

DOI: 10.54254/2755-2721/2027.39074

Comparison of vegetation cover and soil erosion modulus maps indicates that high vegetation cover generally corresponds to weak soil erosion. The overall temporal trend is characterized by initial alleviation and subsequent degradation. From 2000 to 2005, vegetation cover dropped in northern southeastern Hubei and aggravated local erosion, while rising vegetation cover in the southwest reduced erosion risk. Widespread vegetation improvement occurred from 2005 to 2010, especially along rivers and lakes. However, vegetation degradation happened during 2010–2015 due to rapid urbanization. Between 2015 and 2020, vegetation cover rose and erosion eased only in southern Huangshi; most of southeastern Hubei suffered vegetation loss.

3.1.5. Analysis of soil-erosion influencing factors

As illustrated in Figure 6, spatially, the soil-erodibility factor (K) presents relatively high values in the western and northern parts of southeastern Hubei, while low values are observed in the southern and eastern regions. The central-eastern area shows obvious zonal distribution with intermediate K values. Combined comparison with land-use types indicates that cropland and built-up land generally have strong soil erodibility and high K values. Reservoirs, rivers and lakes exhibit moderate values, whereas forest land and unused land feature relatively weak soil erodibility.

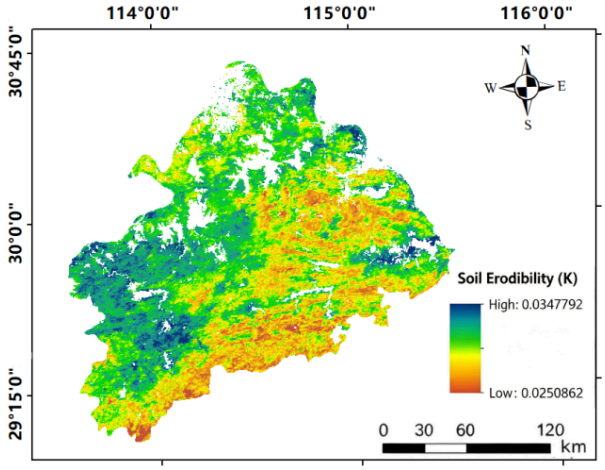

Figure 7. Schematic diagram of soil erosion factors in the study area

3.2. Spatiotemporal variation characteristics of soil erosion in southeastern Hubei

3.2.1. Temporal variation characteristics

In this study, soil erosion grade datasets since 1998 were adopted to analyze the temporal features of soil erosion in southeastern Hubei. The table 2 which shows the classification table of soil erosion grades and the table 3 which shows the transition matrix from 2000 to 2020 were generated for Wuhan, Xianning, Huangshi, Ezhou and their subordinate counties and districts. Overall, soil erosion in southeastern Hubei exhibited a trend of deterioration first and then mitigation.

According to Table 2, slight erosion dominated across the entire study area, followed by light, moderate, strong, very-strong and severe erosion in sequence. Table 2 reveals that soil erosion in 2000 was dominated by slight and light erosion, accounting for 79.78% and 18.4% of the total eroded area, respectively. Compared with 2000, the areas of slight and light erosion increased in

DOI: 10.54254/2755-2721/2027.39074

2005, reaching 81.3% and 16.91%, while the proportion of moderate erosion decreased from 1.63% to 1.58%.

However, this trend only lasted until 2005. Changes occurred during 2005–2010: severe erosion appeared for the first time in the study area, although its proportion was small (0.1% of the total area). The proportion of slight erosion dropped to 77%, while the proportions of light, moderate and strong erosion increased obviously. The proportion of moderate erosion rose from 16.9% to 17.3%, and strong erosion increased remarkably from 0.19% to 0.7%.

The pattern changed again in 2015. Severe erosion disappeared, and the proportion of slight erosion increased sharply, occupying 94% of the total eroded area, whereas other erosion intensities only accounted for a small fraction. By 2020, the proportion of slight erosion decreased substantially to 68.4%, hitting the lowest value within the study period. Meanwhile, the proportion of very-strong erosion reached a historic high of 10%.

Table 2. Soil erosion grade

	2000		2005		2010		2015		2020	
Erosion grade	Area /km^2	Proportion (%)	Area/km^2	Proportion (%)	Area/km^2	Proportion (%)	Area/km^2	Proportion (%)	Area/km^2	Proportion (%)
slight erosion	19750.61	79.7%	20147.11	81.3%	19081.52	77%	23462.83	94.68%	16972.64	68.49%
light erosion	4559.74	18.40%	4190.50	16.91%	4237.58	17.1%	1035.85	4.18%	3387.59	13.67%
moderate erosion	403.93	1.63%	391.54	1.58%	1253.93	5.06%	203.21	0.82%	1747.07	7.05%
strong erosion	39.65	0.16%	47.08	0.19%	173.47	0.7%	52.04	0.21%	213.12	0.86%
very-strong erosion	27.26	0.11%	4.95	0.02%	2.48	0.01%	24.78	0.1%	2458.29	9.92%
severe erosion	0	0	0	0	24.78	0.1%	0	0	0	0
total		100%		100%		100%		100%		100%

3.2.2. Transition matrix of soil erosion grades

A soil erosion grade transition matrix was adopted to explore soil erosion dynamics from 2000 to 2020 [13]. The matrix takes erosion grades in 2000 as the initial state and those in 2020 as the final state. Diagonal values represent unchanged erosion areas and spatial stability; off-diagonal values indicate grade conversions. Transitions from high to low erosion grades imply effective conservation and ecological recovery, while reverse shifts stand for aggravated erosion.

Slight erosion had the largest unchanged area and highest stability owing to gentle terrain, sound vegetation cover and strong anti-erosion capacity, barely disturbed by rainfall and natural variations. By contrast, severe and very-strong erosion areas had small stable zones and poor stability, presenting bidirectional changes: some recovered via ecological restoration, whereas others deteriorated under external disturbances.

Generally, regional soil erosion improved from 2000 to 2020. Extensive moderate, strong and very-strong erosion converted to light or slight erosion, shrinking erosion scope and intensity. Such benefits originated from ecological measures including the Grain-for-Green Program, vegetation

DOI: 10.54254/2755-2721/2027.39074

restoration and small watershed management. Increased fractional vegetation cover improved topsoil structure and water retention, limiting large-scale soil loss.

Nevertheless, local erosion degradation occurred. Some slight and light erosion areas shifted to moderate or strong erosion, driven by urban expansion, road construction and irrational reclamation. Steep-slope farming damages vegetation, and rainfall easily triggers new soil loss.

In summary, soil erosion exhibited obvious spatiotemporal characteristics: overall improvement with local deterioration. Reduced high-intensity erosion area and expanded stable low-grade erosion area verify conservation achievements. Human-induced erosion needs continuous concern. Long-term ecological projects, optimized land use and strict controls on anthropogenic erosion are essential to sustain restoration outcomes.

Table 3. Soil erosion transfer matrix

	Erosion grade/km^2	Slight erosion	light erosion	moderate erosion	strong erosion	very-strong erosion	total/km^2	Proportion (%)
2000	Slight erosion	16932.47	1784.51	85.44	46.96	901.23	19750.61	79.7%
	light erosion	41.88	1603.04	1624.28	28.93	1261.61	4559.74	18.40%
	moderate erosion	0	0	37.51	137.16	228.88	403.93	1.63%
	strong erosion	0	0	0	0.09	39.56	39.65	0.16%
	very-strong erosion	0	0	0	0	27.26	27.26	0.11%
	total	16972.64	3387.59	1747.07	213.12	2458.29	24781.19	100%
	Proportion (%)	68.49	13.67	7.05	0.86	9.92	100%	

3.2.3. Spatial variation characteristics

Spatially, soil erosion intensity rises from the northwest to southeast. The severest erosion zones distribute zonally in central and southeastern regions. In 2000, slight, light and moderate erosion prevailed, with peak erosion in the southeast. The northwest was mainly slight erosion, apart from scattered moderate patches. Erosion intensified in 2005, as southeast moderate erosion shifted to strong erosion.

2010 marked a critical turning point. The 2010 erosion map reveals sharply increased erosion intensity in the southeast and expanding strong erosion spreading toward central and southwest areas. Scattered very-strong and severe erosion patches emerged in southern and southeastern zones. Conditions recovered greatly in 2015, and most of southeastern Hubei returned to slight and light erosion. In 2020, erosion's spatial extent was larger than that in 2000 and 2005, while its intensity dropped compared with 2010 and 2015, especially in central and southeastern regions.And the figure 8 shows the erosion progress from 2000 to 2020.

In summary, historical mining damaged vegetation and terrain and triggered severe erosion in southeastern Hubei [5]. Rapid urbanization led to overexploitation, transforming forests and grasslands into cropland and built-up land. Vegetation loss aggravates soil loss. Meanwhile, growing rainfall volume and intensity boost topsoil erosion. Based on 20-year land-use and fractional vegetation cover data, ecological practices including mine rehabilitation and the Grain-for-Green Program have mitigated erosion. Targeted governance should prioritize the severely eroded southeast. Widespread slight and moderate erosion requires long-term monitoring and ecological management.

DOI: 10.54254/2755-2721/2027.39074

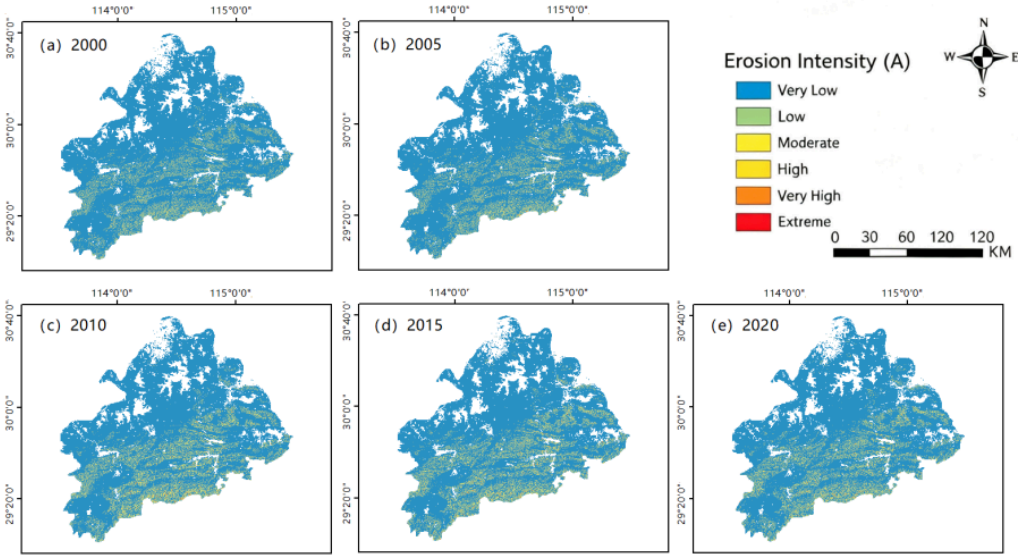

Figure 8. Soil erosion modulus

4. Conclusion and outlook

4.1. Conclusion

Southeastern Hubei's soil erosion experienced deterioration and then alleviation. In 2000, slight and light erosion dominated the region. Erosion worsened in 2005 but stayed within slight, light and moderate grades. A sharp erosion peak occurred in 2010 with rapid growth of moderate and strong erosion. Despite intensity declines from 2015 to 2020, the 2020 erosion level remained higher than in 2000, indicating a long-term worsening trend.

Hilly areas in the southwest and north-central parts are erosion hotspots. Slope grades distribute evenly across this hilly region. Slopes below 15° feature slight to moderate erosion with no severe erosion. The 15°–25° slopes are dominated by moderate erosion, where severe erosion starts to appear. On slopes steeper than 25°, strong and very-strong erosion accounts for 75% of regional total severe erosion area. Erosion intensity increases with slope gradient; steep mountainous zones in the north, southeast and southwest are susceptible to soil loss during heavy rainfall.

Forestland is the main land-use type, followed by cropland and water bodies. Slight and light erosion covers 67.48% of the study area, whereas very-strong and severe erosion occupy under 5%. Cropland is mostly affected by slight and light erosion but includes all erosion grades, contributing 80% of regional severe erosion area.

Fueled by urbanization, ecological land conversion and rising rainfall, soil erosion in southeastern Hubei remains severe and needs administrative attention. Future conservation should prioritize afforestation on steep slopes and sustained management for slight and moderate erosion zones. As a critical erosion-control area, cropland requires targeted measures including terraces and the Grain-for-Green Program to reduce regional soil loss.

DOI: 10.54254/2755-2721/2027.39074

4.2. Outlook

Based on the RUSLE model, this study analyzed soil erosion spatiotemporal changes in southeastern Hubei from 1998 to 2020 and identified how precipitation, topography, vegetation and land use affect soil erosion. However, this research has some limitations. The P-factor (support practice factor) was assigned based only on land-use types, which cannot finely capture local differences in engineering measures like terraces and mine restoration. Besides, NDVI data between 1998 and 2014 were estimated by regression equations, bringing deviations from real vegetation conditions [14].

For future work, field soil sampling and slope surveys can help localize RUSLE parameters and raise the accuracy of soil erosion modulus simulation. Moreover, the geographical detector model [15] can be adopted to quantify factor interactions. Multi-scenario simulation can predict erosion trends under different development paths such as urban expansion and the Grain-for-Green Program. The research scale can also be downscaled to the county level to assess soil loss risks for diverse geographic units, including low hills, mining areas and urban fringes. Such improvements will deliver finer scientific support for mine management, farmland protection and territorial ecological restoration in southeastern Hubei [16].

References

[1] Yang, Y. P., Tian, P., Shen, C. Z., et al. (2024). Soil erosion vulnerability assessment in southwestern Hubei Province based on RUSLE model and geographical detector. *Journal of Soil and Water Conservation, 38*(1), 91-103. DOI:10.13870/j.cnki.stbcxb.2024.01.015.

[2] Tu, Y. (2025). *Spatiotemporal variation of soil erosion and its influencing factors in Hubei Province* [D]. Hubei Minzu University. DOI:10.27764/d.cnki.ghbmz.2025.000352.

[3] Tian, P., Wang, Z., Yu, H. J., et al. (2023). Quantitative evaluation of spatiotemporal pattern and influencing factors of soil and water loss in hilly area of northwestern Hubei. *Research of Soil and Water Conservation, 30*(3), 76-85. DOI:10.13869/j.cnki.rswc.2023.03.054.

[4] Yang, M. M. (2022). *Calculation of global soil erodibility factor (K) and analysis of gravel effect* [D]. Northwest University. DOI:10.27405/d.cnki.gxbdu.2022.001387.

[5] Li, X. B., Hao, S. S., Liu, S. S. (2022). Influence analysis of DEM with different resolutions on topographic factors and soil erosion intensity evaluation: A case study of Peijiamao small watershed in loess hilly and gully region. *Soil and Water Conservation in China*(10), 20-24. DOI:10.14123/j.cnki.swcc.2022.0246.

[6] Hawker, L., Uhe, P., Paulo, L., et al. (2022). A 30 m global map of elevation with forests and buildings removed. *Environmental Research Letters, 17*(2), 024016. https://doi.org/10.1088/1748-9326/ac4d4f.

[7] Zhang, X. X., Zhang, J. Y., He, P., et al. (2026). Soil erosion risk and prediction under land use changes based on RUSLE and PLUS models in the black soil region of Northeast China. *CATENA, 272*, 110371. https://doi.org/10.1016/j.catena.2026.110371.

[8] Xu, L. Y., Guo, W. L., & Jia, J. A. (2024). Spatiotemporal variation and driving factors of soil erosion in hilly area of southeast China: A case study of Zhangjiajie City, Hunan Province. *Bulletin of Soil and Water Conservation, 44*(1), 218-226+237. DOI:10.13961/j.cnki.stbctb.2024.01.022.

[9] Wang, J., Yang, J., Li, Z., et al. (2025). Research on soil erosion based on remote sensing technology: A review. *Agriculture, 15*(1), 18. https://doi.org/10.3390/agriculture15010018.

[10] Sun, Z. J., Hu, X. P., He, B. X., et al. (2025). Coupling coordination and driving factors of soil erosion and rocky desertification in karst area of Lichuan City. *Journal of Forest and Grassland Resources*(1), 126-136. DOI:10.13466/j.cnki.lczyyj.2025.01.014.

[11] Ashatkin, I. A., Maltsev, K. A., Gainutdinova, G. F., et al. (2020). Analysis of relief morphometry by global DEM in the southern part of the European territory of Russia. *Uch. Zap. Kaz. Univ. Ser. Estestv. Nauki, 162*(4), 612-628. https://doi.org/10.26907/2542-064X.2020.4.612-628.

[12] Liao, R. E., Qi, S., Lai, J. L., et al. (2024). Spatiotemporal variation and driving forces of hydraulic erosion in alpine and gorge region of southwest China. *Research of Soil and Water Conservation, 31*(5), 139-147. DOI:10.13869/j.cnki.rswc.2024.05.002.

DOI: 10.54254/2755-2721/2027.39074

[13] Wang, W. Z., & Jiao, J. Y. (1996). Study on quantitative assessment of soil erosion factors in China. *Bulletin of Soil and Water Conservation*(5), 1–20. DOI:10.13961/j.cnki.stbctb.1996.05.001.
[14] Wu, H. Y., Xiong, J. F., Hou, X., et al. (2023). 2001–2020 soil water erosion dataset for Northeast China. *China Scientific Data, 8*(4), 290–304.
[15] Wang, J. F., & Xu, C. D. (2017). Geodetector: Principle and prospective. *Acta Geographica Sinica, 72*(1), 116–134. DOI:10.11821/dlxb201701010.
[16] Deng, Z. Q., & Liu, C. L. (2025). Analysis of soil erosion and sensitivity in Jiangxi Province based on geographical detector. *Journal of Irrigation and Drainage*(7), 8–14. DOI:10.12396/jsgg.2025016.